

EFFICIENT CODING OF 360° VIDEOS EXPLOITING INACTIVE REGIONS IN PROJECTION FORMATS

Christian Herglotz¹, Mohammadreza Jamali¹, Stéphane Coulombe¹, Carlos Vazquez¹, Ahmad Vakili²

¹École de technologie supérieure, Montréal

² Summit Tech Multimedia, Montréal

ABSTRACT

This paper presents an efficient method for encoding common projection formats in 360° video coding, in which we exploit inactive regions. These regions are ignored in the reconstruction of the equirectangular format or the viewport in virtual reality applications. As the content of these pixels is irrelevant, we neglect the corresponding pixel values in rate-distortion optimization, residual transformation, as well as in-loop filtering and achieve bitrate savings of up to 10%.

Index Terms— 360 degree, video coding, inactive areas, HEVC, octahedron, icosahedron, segmented sphere, rotated sphere, cubemap, projection

1. INTRODUCTION

In recent years, virtual reality (VR) applications went through a remarkable evolution such that nowadays, many portable devices can process these applications in real time. A common example for a VR application is 360° video playback. In this application, the user wears a headset with the portable device attached, where the display is used to create a simulated environment in which the user immerses. Turning his head in all directions, he can then see what happens around him in that environment.

In this application, video data needs to be recorded and saved in a special projection format to cover all potential viewing angles [1]. This video data is commonly called 360° video and overcomes the drawback of classic equilinear sequences, which usually cover less than 180° of viewing angle horizontally and vertically, in a single point of view. To this end, a high number of different projection formats have been proposed and studied [2, 3, 4]. The target of a projection format is to optimize the user experience which is measured in terms of the visually perceived quality, independent from the viewing angle [5].

In all these projection formats, the visual data is packed into a rectangular pixel array that can then be compressed with standard compression standards like H.264 [6] or HEVC [7]. After decoding, the pixel data is used to undo the projection by calculating the underlying sphere or the viewport, which is then shown to the user. This method provides the advantage that most modern smartphones and portable devices

are capable of decoding the visual data and performing subsequent reconstruction in real time because dedicated video decoding hardware is available.

Depending on the projection format, the projected visual data can have different properties. For example, the common equirectangular projection (ERP) distorts straight lines in a conventional equilinear projection to curves [1]. If a projection is used that keeps straight lines like Cubemap (CMP), the video data is projected onto rectangular or triangular faces. These faces are packed into the rectangular pixel array such that either discontinuities appear at the face borders, or regions with inactive sample data occur that are not needed for the proper reconstruction of the video. In [8], the effect of different projections on compression efficiency and computational complexity is studied.

This paper tackles the encoding method for projection formats containing inactive samples. Therefore, we modify the encoding process as follows. First, during the rate-distortion optimization (RDO), which determines the best prediction and coding parameters [9], we propose to neglect the distortion imposed by pixels in inactive regions. Second, we propose to set the inactive residual coefficients to zero. Third, we neglect the inactive samples when collecting statistics for the best sample adaptive offset (SAO) post-processing filter [10]. The evaluation shows that without degrading the visual quality, average bitrate savings between 0.3% and 6% can be achieved in HEVC, depending on the projection format.

This paper is organized as follows. First, Section 2 reviews projection formats and presents related work on 360° video coding. Afterwards, we present the proposed coding method in detail in Section 3, show the evaluation setup in Section 4, and evaluate the performance in Section 5. Finally, Section 6 concludes this paper.

2. INACTIVE REGIONS IN 360° VIDEOS

In the beginning of 360° video coding, only few projection formats were considered. For example, in standardization, the first attempts to standardize 360° video handling only considered ERP and CMP [11]. Later on, with the establishment of the joint video exploration team (JVET), more projection formats were developed and studied to find the one best suited for efficient compression in the rate-distortion sense

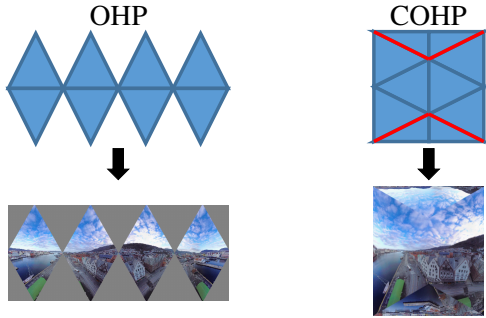


Fig. 1. Packing of triangular faces in octahedron projection. On top, the location of the faces is shown, the bottom shows an example of a projected frame of the AerialCity sequence.

[2]. Therefore, a dedicated software was written that is able to convert between all considered projection formats [12] and evaluate their compression performance in a unified manner.

For all the projection formats considered in this paper, the visual information is projected onto multiple faces. These faces are then packed into a rectangular frame. An example for two different packing methods is depicted in Fig. 1. It shows octahedron projection (OHP), in which the input sphere is projected onto an octahedron consisting of eight triangles. On the left, a rectangular format is obtained by padding the spaces around the OHP faces with gray pixels. In compact octahedron (COHP) on the right, the triangles are packed more densely such that no gray area remains. However, on some borders between the triangles, the content is discontinuous as indicated by the red lines. In this case, 16 samples are added between the faces to smooth the transition and hence reduce the coding bitrate [12]. In the proposed algorithm, both kinds of inactive pixels are considered to improve the compression efficiency.

The segmented sphere projection (SSP) segments the sphere into three tiles: north pole, equator and south pole [3]. The boundaries of the three segments are 45°N and 45°S. The top and bottom segments (north and south poles) are mapped into two circles. The middle part (the equatorial segment) follows the same mapping as ERP and is projected onto a rectangle. The diameter of the circle is equal to the width of the equatorial segment because both polar segments and equatorial segment have a 90° latitude span [3]. SSP spends fewer pixels at the polar segments compared to ERP which helps improving the coding efficiency. However, the circular faces are padded with inactive samples.

In icosahedron projection (ISP), there are 20 triangular faces which are packed in a compact format (CISP). To compact the 20 triangles in a rectangular frame, some triangles are split or flipped vertically or horizontally [4].

The rotated sphere projection (RSP) consists of two faces which are compacted in a rectangular frame in two rows. The top face is obtained from the middle part of ERP which includes the range of 270° horizontally and 90° vertically. The

bottom face covers the same range. However, the basic sphere to obtain ERP is rotated 180° along the Y-axis and 90° along the X-axis.

Various works improve padding techniques for the inactive regions to increase the compression performance. He et al. propose a dedicated technique for discontinuous borders and report bitrate reductions between 0.3% and 4.3% [13]. Yoon et al. propose a technique for SSP [3] with bitrate reductions of 0.3%. Kim et al. propose a suitable technique when introducing the icosahedron projection [4].

Other work explicitly targeting discontinuous borders was done by Sauer et al. [14]. They target the deblocking filter in CMP and modify the process when the block border is located on a discontinuity. They show that coding artifacts can be reduced significantly. Work targeting ERP projections was done by Budagavi et al. [15] performing region adaptive smoothing, in which up to 20% of bitrate could be saved. In a similar direction, Li et al. proposed to use spherical-domain RDO to distribute the available bandwidth more evenly [16] such that more than 10% of bits could be saved at the same visual quality. To the best of our knowledge, the proposed method is the first that neglects the distortion of inactive samples during encoding.

3. PROPOSED ALGORITHM

To implement the proposed algorithm, we modify the HEVC reference software version HM-16.20 [17]. It is required to signal the encoder the locations of the inactive samples. As these locations do not change over time, it is sufficient to signal a binary mask at input resolution indicating whether a pixel is active ('1') or not ('0'). For each tested projection and resolution, such a mask is generated and signaled to the encoder. The following three subsections explain the modifications in distortion calculation, residual error transformation, and SAO handling, which can also be adapted for other coding standards.

3.1. Distortion Calculation

In HM-16.20, rate-distortion optimization (RDO) is applied to find the best coding mode and coding parameters. Depending on this mode, three different kinds of distortion metrics are calculated: the sum of absolute differences (SAD), the sum of squared differences (SSD), and the sum of absolute Hadamard transformed differences (SATD). Assume that an original block B and a distorted block \tilde{B} , defined for the set of pixel positions \mathcal{P} , are given. The distortion D in terms of SSD is then calculated as

$$D = \sum_{\mathbf{m} \in \mathcal{P}} \left(B(\mathbf{m}) - \tilde{B}(\mathbf{m}) \right)^2, \quad (1)$$

with \mathbf{m} a 2D pixel index.

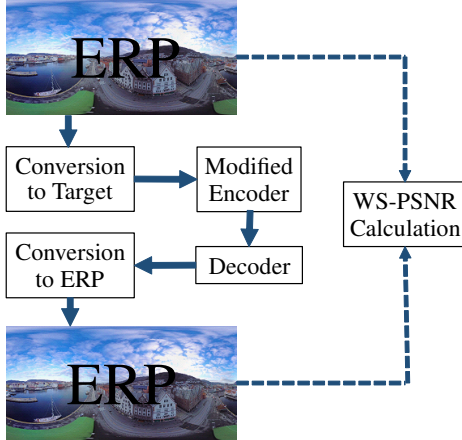


Fig. 2. Evaluation procedure for the proposed encoding method. All distortion calculations are performed in equirectangular domain. The target is one of the projection formats shown in Table 2.

We assume that the block includes a set of inactive samples \mathcal{I} , which is a subset of \mathcal{P} . We now calculate the distortion as

$$D_{\text{mod}} = \sum_{\mathbf{m} \in \{\mathcal{P} \setminus \mathcal{I}\}} \left(B(\mathbf{m}) - \tilde{B}(\mathbf{m}) \right)^2. \quad (2)$$

For SAD, the distortion calculation is modified accordingly. For SATD, before the Hadamard transform, the sample difference of inactive samples is set to zero.

3.2. Residual Coefficient Handling

After prediction of a block, the residual error is determined and transformed with a discrete cosine transform (DCT) [18], where the residual error is the difference between the original block and the predicted block. We propose a straightforward method to reduce the number of bits needed to code the residual coefficients in the DCT domain. The block of spatial domain residual coefficients R is calculated by

$$R(\mathbf{m}) = B(\mathbf{m}) - \hat{B}(\mathbf{m}), \quad \forall \mathbf{m} \in \mathcal{P}, \quad (3)$$

where B is the block of original pixel values and \hat{B} the block of predicted pixel values.

After this operation and before transformation, we set all values in the set of inactive samples \mathcal{I} to zero as

$$R(\mathbf{m}) = 0, \quad \forall \mathbf{m} \in \mathcal{I}. \quad (4)$$

This operation minimizes the power of the residual signal, which also minimizes the power of the signal in the transform domain such that fewer bits are needed to code the residual coefficients.

Table 1. Sequences used for algorithm evaluation. All sequences are coded in YUV420 format with a bit depth of 8. The Balboa sequence has a frame rate of 60 fps, the other sequences 30 fps.

	Resolution	Sequences
4K	3840 × 1920	AerialCity, PoleVault
6K	6144 × 3072	Balboa, Landing2
8K	8192 × 4096	Gaslamp, Trolley

3.3. Sample Adaptive Offset

In the HM-16.20 encoder, each coding tree unit (CTU) is tested for the sample adaptive offset filter (SAO) as introduced in [10]. Therefore, statistics are collected for all pixels by classifying them in the categories band offset (BO) and edge offset (EO), depending on their band and edge type.

As explained in [10], the band or the edge category of a pixel value is obtained as a function of the pixel value itself and adjacent pixel values. For edge offset, horizontal, vertical, or diagonal directions are considered. Then, for each category, a counter and the overall sum of the differences between the original and the reconstructed pixel values is defined. Depending on the categorization, the counter is incremented and the overall difference updated. The SAO parameters are then chosen to minimize the overall difference. In the proposed method, the categorization, the increment, and the addition to the overall difference are skipped if the pixel is located in an inactive region. However, an inactive sample adjacent to an active sample can be used to determine the category of the active sample.

4. EVALUATION SETUP

The framework depicted in Fig. 2 is used for performance evaluation. For conversion and distortion calculation, we use 360Lib [19] which introduces four new objective quality metrics in addition to the traditional PSNR: WS-PSNR, CPP-PSNR, S-PSNR-NN and S-PSNR-I [2]. In this work, we use WS-PSNR to calculate the Bjøntegaard-Delta rate (BD-Rate) [20] which shows the average bitrate savings.

WS-PSNR calculates the PSNR based on distortions for all pixels on the rectangular frame. However, unlike traditional PSNR, distortions are weighted based on the pixels positions. The weights are calculated based on the spherical areas which each pixel take on the sphere. It should be noted that the two frames which are used for WS-PSNR computations must have the same resolution and projection format.

We tested six different projection formats on six different test sequences. The test sequences are taken from the JVET common test conditions [2, 21] and are originally provided in the ERP projection format. The main properties are listed in Table 1. The projection formats are taken from [12] and the

Table 2. Projection formats used for algorithm evaluation. 4K, 6K, and 8K in the first line refer to the resolution of the input sequence (see Table 1). Below, the listed resolutions represent the target resolution after projection, and the percentages show the fraction of inactive samples.

Proj.	4K		6K & 8K	
	Resolution	Inact.	Resolution	Inact.
CMP	3840 × 2880	50.0%	4736 × 3552	50.0%
OHP	2880 × 1248	49.7%	6176 × 2672	49.9%
COHP	2176 × 2552	1.25%	2672 × 3128	1.02%
CISP	1416 × 1816	8.71%	2496 × 3320	4.94%
RSP	2880 × 1920	5.33%	3552 × 2368	5.48%
SSP	1008 × 6080	7.64%	1216 × 7328	7.56%

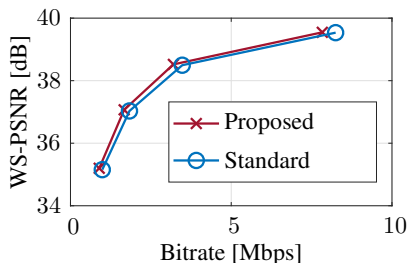


Fig. 3. Rate-distortion curves for the standard (blue) and the proposed (red) encoder. The sequence is AerialCity, the projection format is OHP, and the BD-Rate is -9.77% .

conversion is performed using the 360Lib-7.0 [19]. Depending on the resolution of the input sequence, different output resolutions are chosen as shown in Table 2.

For encoding the projected formats, we use HM-16.20 with the QPs 22, 27, 32, and 37 in the random access configuration [22]. Because of a high simulation time, for all sequences, we code 33 frames to cover two groups of pictures (GOPs) and two I-frames.

5. RATE-DISTORTION PERFORMANCE

Fig. 3 shows the rate-distortion curves for the AerialCity sequence in OHP projection. It can be seen that the curve corresponding to the proposed approach reaches the same WS-PSNR as the standard approach at a smaller bitrate.

The results for all sequences and all projection formats are summarized in Table 3. We can see that on average, all projection formats achieve significant bitrate savings. Highest savings can be observed for the OHP projection (up to 10%). The reason is that in this projection format, the border between active and inactive samples crosses the coding block structure diagonally. As a consequence, the prediction needs to compromise between an accurate prediction of the

Table 3. BD-Rate savings in terms of WS-PSNR [%].

Sequence	Projection Format					
	CMP	OHP	COHP	CISP	RSP	SSP
AerialCity	0.60	9.77	0.85	3.05	0.63	0.94
PoleVault	0.15	4.10	0.36	2.16	0.02	0.23
Balboa	0.44	8.16	1.55	2.76	0.41	0.89
Landing2	0.26	6.91	1.65	3.22	0.48	1.24
Gaslamp	0.19	4.78	0.76	1.16	0.26	0.37
Trolley	0.15	2.39	0.36	0.78	0.09	0.21
Average	0.30	6.02	0.92	2.19	0.32	0.65

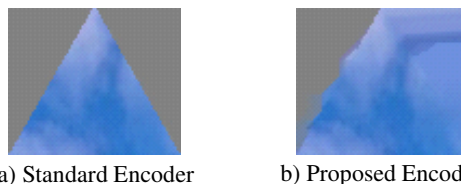


Fig. 4. Zoomed samples of the AerialCity sequence in OHP format after decoding for the standard (a) and the proposed encoder (b). The cutouts are taken from the first frame, top left face, coded with QP 22. The face shows the sky.

edge and an accurate prediction of the active area, which in general leads to large residuals that are costly to code. The proposed method removes the need to reconstruct the edge such that bitrate can be saved.

A visual comparison between the visual data supports this finding (Fig. 4). One can see that the original method reconstructs the gray area with a high quality. In the proposed method, the corresponding region on the right mainly shows predicted pixel values from an angular prediction mode. Hence, bits to code the residual are saved.

6. CONCLUSIONS

This paper presented an encoding method that disregards pixels in inactive areas. The method is applicable to many 360° projection formats and can be used for other formats in which inactive areas occur. Our evaluation indicates that the proposed method provides bitrate savings up to 10%.

In future work, inactive regions can be exploited for encoder speedup. Studying the separate impact of distortion, residual, and SAO handling would also be interesting. Further projection formats like fisheye video can also be tested.

Acknowledgment

This work was supported by Mitacs Canada and Summit Tech Multimedia (<https://www.summit-tech.ca/>).

7. REFERENCES

- [1] F. Nielsen, "Surround video: a multihead camera approach," *The Visual Computer*, vol. 21, no. 1, pp. 92–103, Feb. 2005.
- [2] J. Boyce, E. Alshina, A. Abbas, and Y. Ye, "JVET common test conditions and evaluation procedures for 360° video," AHG Report, JVET-E1030, Joint Video Exploration Team (JVET) of ITU-T SG 16 WP 3 and ISO/IEC JTC 1/SC 29/WG 11, Jan. 2017.
- [3] Y.-U. Yoon, Y.-J. Ahn, D. Sim, and J.-A. Kim, "Efficient methods of inactive regions padding for segmented sphere projection (SSP) of 360 video," *IEICE Transactions on Information and Systems*, vol. 101, no. 11, pp. 2836–2839, 2018.
- [4] H.-H. Kim, Y.-U. Yoon, and J.-A. Kim, "An efficient frame packing method for icosahedral projection in 360 video coding," *IEIE Transactions on Smart Processing & Computing*, vol. 7, no. 3, pp. 195–200, 2018.
- [5] X. Xiu, Y. He, Y. Ye, and B. Vishwanath, "An evaluation framework for 360-degree video compression," in *Proc. IEEE Visual Communications and Image Processing (VCIP)*, Dec. 2017, pp. 1–4.
- [6] *Advanced Video Coding for Generic Audio-Visual Services*, ITU-T Rec. H.264 and ISO/IEC 14496-10 (AVC), ITU-T and ISO/IEC JTC 1, Apr. 2003.
- [7] *High Efficiency Video Coding*, ITU-T Rec. H.265 and ISO/IEC 23008-2, ITU-T and ISO/IEC JTC 1/SC 29/WG 11 (MPEG), Apr 2013.
- [8] M. Jamali, F. Golaghazadeh, S. Coulombe, A. Vakili, and C. Vazquez, "Comparison of 3D 360-degree video compression performance using different projections," in *Proc. IEEE Canadian Conference on Electrical and Computer Engineering (CCECE)*, May 2019.
- [9] G.J. Sullivan and T. Wiegand, "Rate-distortion optimization for video compression," *IEEE Signal Processing Magazine*, vol. 15, no. 6, pp. 74–90, Nov. 1998.
- [10] C.-M. Fu, E. Alshina, A. Alshin, Y.-W. Huang, C.-Y. Chen, C.-Y. Tsai, C.-W. Hsu, S.-M. Lei, J.-H. Park, and W.-J. Han, "Sample adaptive offset in the HEVC standard," *IEEE Transactions on Circuits and Systems for Video Technology*, vol. 22, no. 12, pp. 1755–1764, Dec. 2012.
- [11] R. Skupin, Y. Sanchez, Y. Wang, M. M. Hannuksela, J. Boyce, and M. Wien, "Standardization status of 360 degree video coding and delivery," in *Proc. IEEE Visual Communications and Image Processing (VCIP)*, Dec. 2017, pp. 1–4.
- [12] Y. Ye and J. Boyce, "Algorithm descriptions of projection format conversion and video quality metrics in 360lib version 7," JVET-K1004, Joint Video Exploration Team (JVET) of ITU-T SG 16 WP 3 and ISO/IEC JTC 1/SC 29/WG 11, July 2018.
- [13] Y. He, Y. Ye, P. Hanhart, and X. Xiu, "Geometry padding for motion compensated prediction in 360 video coding," in *Proc. Data Compression Conference (DCC)*, Apr. 2017, p. 443.
- [14] J. Sauer, M. Wien, J. Schneider, and M. Bläser, "Geometry-corrected deblocking filter for 360° video coding using cube representation," in *Proc. Picture Coding Symposium (PCS)*, June 2018, pp. 66–70.
- [15] M. Budagavi, J. Furton, G. Jin, A. Saxena, J. Wilkinson, and A. Dickerson, "360 degrees video coding using region adaptive smoothing," in *Proc. IEEE International Conference on Image Processing (ICIP)*, Sep. 2015, pp. 750–754.
- [16] Y. Li, J. Xu, and Z. Chen, "Spherical domain rate-distortion optimization for 360-degree video coding," in *Proc. IEEE International Conference on Multimedia and Expo (ICME)*, July 2017, pp. 709–714.
- [17] Joint Collaborative Team on Video Coding, "HEVC test model reference software (HM)," <https://hevc.hhi.fraunhofer.de/>, [accessed 2019-02].
- [18] G.J. Sullivan, J. Ohm, Woo-Jin Han, and T. Wiegand, "Overview of the high efficiency video coding (HEVC) standard," *IEEE Transactions on Circuits and Systems for Video Technology*, vol. 22, no. 12, pp. 1649–1668, Dec. 2012.
- [19] Joint Video Exploration Team, "360lib projection format conversion software," <https://jvet.hhi.fraunhofer.de/svn/svn.360Lib/>, [accessed 2019-02].
- [20] G. Bjøntegaard, "Calculation of average PSNR differences between RD curves," document, VCEG-M33, Austin, TX, USA, Apr. 2001.
- [21] P. Hanhart, J. Boyce, and K. Choi, "JVET common test conditions and evaluation procedures for 360° video," JVET-K1012, Joint Video Exploration Team (JVET) of ITU-T SG 16 WP 3 and ISO/IEC JTC 1/SC 29/WG 11, July 2018.
- [22] F. Bossen, "JCTVC-L1100: Common test conditions and software reference configurations," Tech. Rep., Joint Collaborative Team on Video Coding (JCT-VC) of ITU-T SG16 WP3 and ISO/IEC JTC1/SC29/WG11, Geneva, Switzerland, Jan. 2013.